Hindawi Publishing Corporation
Journal of Nanomaterials
Volume 2016, Article ID 9425289, 10 pages
http://dx.doi.org/10.1155/2016/9425289

Research Article

PLGA/Nano-ZnO Composite Particles for Use in Biomedical Applications: Preparation, Characterization, and Antimicrobial Activity

Ana Stanković,[1] Meltem Sezen,[2] Marina Milenković,[3] Sonja Kaišarević,[4] Nebojša Andrić,[4] and Magdalena Stevanović[1]

[1]*Institute of Technical Sciences of the Serbian Academy of Sciences and Arts, Belgrade, Serbia*
[2]*Sabanci University Nanotechnology Research and Application Center (SUNUM), Orhanli Tuzla, Istanbul, Turkey*
[3]*Departments of Microbiology and Immunology, University of Belgrade, Faculty of Pharmacy, Belgrade, Serbia*
[4]*Department of Biology and Ecology, University of Novi Sad, Faculty of Sciences, Novi Sad, Serbia*

Correspondence should be addressed to Magdalena Stevanović; magdalena.stevanovic@itn.sanu.ac.rs

Received 25 July 2016; Revised 8 November 2016; Accepted 21 November 2016

Academic Editor: R. Torrecillas

Copolymer poly (DL-lactide-co-glycolide) (PLGA) is extensively investigated for various biomedical applications such as controlled drug delivery or carriers in the tissue engineering. In addition, zinc oxide (ZnO) is widely used in biomedicine especially for materials like dental composites, as a constituent of creams for the treatment of a variety of skin irritations, to enhance the antibacterial activity of different medicaments and so on. Uniform, spherical ZnO nanoparticles (nano-ZnO) have been synthesized via microwave synthesis method. In addition to obtaining nano-ZnO, a further aim was to examine their immobilization in the PLGA polymer matrix (PLGA/nano-ZnO) and this was done by a simple physicochemical solvent/nonsolvent method. The samples were characterized by X-ray diffraction, scanning electron microscopy, laser diffraction particle size analyzer, differential thermal analysis, and thermal gravimetric analysis. The synthesized PLGA/nano-ZnO particles are spherical, uniform, and with diameters below 1 μm. The influence of the different solvents and the drying methods during the synthesis was investigated too. The biocompatibility of the samples is discussed in terms of in vitro toxicity on human hepatoma HepG2 cells by application of MTT assay and the antimicrobial activity was evaluated by broth microdilution method against different groups of microorganisms (Gram-positive bacteria, Gram-negative bacteria, and yeast *Candida albicans*).

1. Introduction

Recently, significant effort has been dedicated to develop micro- and nanoparticles for drug delivery since they offer an appropriate means to distribute the therapeutically active drug molecule only to the site of action, without affecting healthy organs and tissues [1–3]. Many different polymers, both synthetic and natural, have been employed in making biocompatible and biodegradable nanoparticles. Polyesters micro- and nanoparticles are used for the controlled delivery of different classes of active substances such as anticancer agents, growth factors, antibiotics, antimicrobial agents, metal, and metal oxide nanoparticles [4–8]. Polyester, poly (DL-lactide-co-glycolide) (PLGA), is a copolymer approved by Food and Drug Administration (FDA) for medical and pharmaceutical applications. Physicochemical properties of nanoparticles which include small size and very large specific surface area significantly improve their bioavailability and minimize drug toxicity. Inorganic antibacterial nanoparticles especially offer some unique benefits in overcoming major problems related to treatment process such as reducing dosage of antibacterial agent, minimizing side effects, overcoming bacterial resistance, and lowering overall cost of the fabrication process [7, 8].

ZnO represents a multifunctional material with a wide and direct band gap energy of 3,37 eV. Besides its extraordinary optical, catalytic, semiconducting, and piezoelectric properties, ZnO is a promising material for a variety

of biological applications because of its chemical stability, antimicrobial activity, high biocompatibility, and nontoxicity to human cells [9, 10]. Also, zinc is a mineral element essential to human health and used in the form of ZnO in the daily supplement for zinc. As a consequence of previously mentioned properties ZnO nanoparticles can be used for cellular imaging [9, 10], biodetection [11], drug delivery [12, 13], and various kinds of therapy [14, 15]. ZnO has a wide range of different nanostructures already used in numerous commercial products such as sunscreen products, different types of sensors, industrial coatings, and antibacterial agents [16]. Particularly ZnO nanoparticles show a wide range of antibacterial activities towards Gram-positive and Gram-negative bacteria, including a major food borne pathogens attributed to the generation of reactive oxygen species (ROS) on this oxide surfaces. In recent years, much attention has been paid to preparation of organic/nanosized inorganic-particles composite materials for a various types of applications especially in medicine and pharmacy [7, 17]. For example, inorganic core-polymer shell hybrid microspheres have attracted attention because the materials can reveal special characteristics, such as improved strength, shape, and chemical resistance [18]. Above all, the properties of nanocomposites are greatly influenced by both the dispersing degree of nanoparticles in the base polymers and the interfacial adhesion between the inorganic and organic components [19]. Although nanocomposites can be prepared by simply mixing of nanoparticles with base polymers, the dispersing degree of nanoparticles and the interfacial linkage were obviously insufficient to obtain desirable material properties [20].

In previous studies, ZnO was incorporated in variety of different polymers such as poly (methyl methacrylate) [21, 22], polystyrene [23, 24], polyamide [25], polyacrylonitrile [26], and polyurethane [27, 28] and the results have shown that the prepared polymer/ZnO composites presented better performances compared to the polymers alone. All of these composite materials were prepared in the forms of films, scaffolds, fibers, or grafts [29, 30]. For the preparation of these polymer/ZnO composites different methods were applied such as dissolution [31], microemulsion polymerization [24], sonication [32], or spin coating method [33].

Our study thus reports on obtaining innovative PLGA nanocomposite spheres with immobilized nano-ZnO (PLGA/nano-ZnO), which represent an important system in the field of medicine, pharmacy, and controlled drug delivery and in particular to prevent infections. The samples were characterized by X-ray diffraction (XRD), scanning electron microscopy (SEM), laser diffraction particle size analyzer (PSA), differential thermal analysis (DTA), and thermal gravimetric analysis (TGA) which demonstrated the successful immobilization of ZnO nanoparticles within PLGA polymer matrix. Controlling the morphology of micro- and nanoparticles is essential for exploiting their properties for their utilization in different technologies. Therefore, in this study we have examined influence of different solvents as well as method of drying on the morphology of PLGA/nano-ZnO. Further, in order to evaluate the in vitro cytotoxic potential of as prepared ZnO as well as PLGA/nano-ZnO, we used a test system with human hepatoma cells, HepG2. This was done by the 3-(4,5-dimethylthiazol-2-yl)-2,5-diphenyltetrazolium bromide (MTT) assay. The antimicrobial activities of ZnO as well as PLGA/nano-ZnO were evaluated by broth microdilution method against the Gram-positive bacteria *Staphylococcus aureus* (ATCC 25923), *Staphylococcus epidermidis* (ATCC 12228), and *Bacillus subtilis* (ATCC 6633) and the Gram-negative bacteria *Escherichia coli* (ATCC 25922), *Klebsiella pneumoniae* (ATCC 13883), *Salmonella abony* (NTCT – 6017) and *Pseudomonas aeruginosa* (ATCC 27853), and the yeast *Candida albicans* (ATCC 24433).

2. Materials and Methods

2.1. Materials. Poly (DL-lactide-co-glycolide) (PLGA) was obtained from *Durect, Lactel, Adsorbable Polymers International* and had lactide to glycolide ratio of 50 : 50. Molecular weight of polymer was 40000–50000 g/mol. Polyvinylpyrrolidone (PVP), zinc acetate dihydrate ($Zn(CH_3COO)_2{\cdot}2H_2O$), and sodium hydroxide (NaOH) were obtained from *Merck Chemicals Ltd.* (Merck, Germany). All chemicals and solvents were of reagent grade.

2.2. Methods

2.2.1. Synthesis of ZnO Nanoparticles. ZnO nanoparticles were prepared via microwave assisted synthesis method as previously described, but with modifications [34]. Starting chemicals were zinc acetate dihydrate ($Zn(CH_3COO)_2{\cdot}2H_2O$) and sodium hydroxide (NaOH). In the synthesis procedure 1.75 M solution of NaOH was slowly added into a 0.07 mol solution of $Zn(CH_3COO)_2\,2H_2O$ at permanent temperature of 60°C and under continuous stirring at 1000 rpm. The white precipitate was formed, indicating enactment of a chemical reaction. The as prepared suspension was treated in a microwave field through 5 min time period. Strength of the applied microwave field was 150 W. Final reaction product was cooled to the room temperature and then centrifuged at 8000 rpm for 10 min to obtain white precipitate. Synthesized ZnO powder was washed out several times with absolute ethanol and deionized water and dried at 60°C for couple hours.

2.2.2. Synthesis of PLGA/Nano-ZnO Particles with Acetone as Solvent and Ethanol as Nonsolvent. PLGA/nano-ZnO particles were synthesized by physicochemical solvent/nonsolvent method. Immobilization of ZnO nanoparticles into PLGA polymer matrix was performed using a homogenization process of water and organic phase (Figure 1). Firstly, 200 mg of PLGA was dissolved in 10 mL of acetone. This solution was constantly mixed on a magnetic stirrer for about 15 min and at room temperature. Thereafter, 1 mL of the ZnO dispersion in acetone (0.55% w/w) was added dropwise into a PLGA/acetone solution while constantly being homogenized at 1200 rpm for 30 min. This was followed by precipitation by addition of 15 mL ethanol, with the solution obtained being poured very slowly into 40 mL aqueous 0.05% (w/w) PVP solution, with continuous stirring at 1200 rpm. PVP was used as a stabilizer in order to prevent particles agglomeration.

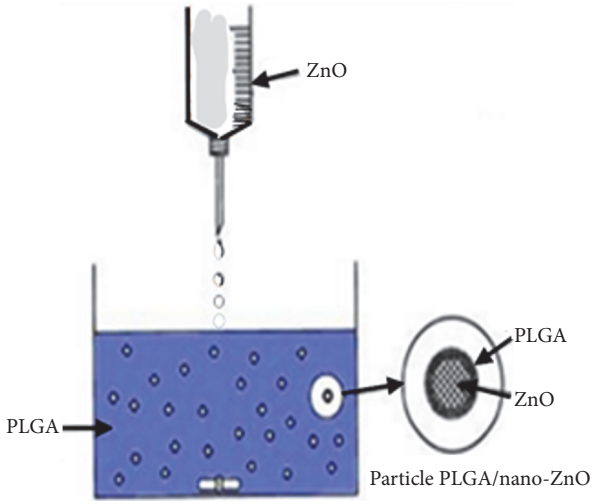

Figure 1: Scheme for preparation of PLGA/nano-ZnO particles.

Finally, the prepared PLGA/nano-ZnO dispersion was decanted and left overnight to dry at room temperature.

2.2.3. Synthesis of PLGA/Nano-ZnO Particles with Ethyl Acetate as Solvent and Ethanol as Nonsolvent. In order to examine the influence of different solvents on morphology of PLGA/nano-ZnO particles, ethyl acetate ($C_4H_8O_2$) was used as solvent in the experiment instead of acetone. PLGA commercial granules (200 mg) were dissolved in 10 mL ethyl acetate over approximately 15 min at room temperature. All other reaction parameters were caped the same as in the experiment described above.

2.2.4. Synthesis of PLGA/Nano-ZnO Particles Using Freeze-Drying in the Synthesis. Freeze-drying or lyophilisation is a method used to transform solutions of formulations into solids of sufficient stability for distribution and storage. Examination of the influence of freeze-drying on morphology of PLGA/nano-ZnO particles was also part of this work. All steps in the synthesis were the same as in the experiments described above except that the PLGA/nano-ZnO particles were freeze-dried. After the freezing, method of lyophilisation was utilized at −55°C and the pressure of 0.3 mbar. Main drying was performed for 8.5 h, and final drying for 30 min, using Freeze Dryer Christ Alpha 1-2/LD plus.

2.2.5. Morphology Studies. To define the microstructure of ZnO particles, field-emission scanning electron microscopy (FE-SEM) analysis was carried out, on a Carl Zeiss SUPRA 35 VP instrument. The size distribution of the synthesized samples was measured using the laser diffraction particle size analyzer (Mastersizer 2000; Malvern Instruments Ltd.). The size measurement range of this instrument is from 20 nm up to 2 mm. Prior to measuring, the sample was treated for 15 min in an ultrasonic bath. The morphology of the synthesized PLGA/nano-ZnO particles was examined using scanning electron microscopy (SEM) on JEOL JIB-4601 F Multi Beam Platform.

2.2.6. XRD Analysis. For identification of the phase composition (phase analysis) of the synthesized powders, X-ray diffraction (XRD) method was applied with a Philips PW 1050 diffractometer with Cu-$K_{\alpha 1,2}$ radiation. The measurements were carried out in the 2θ range of 10° to 70°, with a scanning step width of 0,05° and 2 s per step.

2.2.7. Thermal Analysis. Differential thermal analysis (DTA) and thermal gravimetric analysis (TGA) measurements were carried out using a SETSYS Evolution TGA-DTA/DSC instrument *(SETERAM Instrumentation, France)* on powdered sample PLGA/nano-ZnO of approximately 15 mg. Assigned temperature range was from room temperature to 1200°C. The data were baseline corrected by carrying out a blank run and subtracting this from the original data.

2.2.8. Cytotoxicity Study. The samples were evaluated for their in vitro cytotoxicity towards human hepatoma HepG2 cells by application of MTT assay. This is a colorimetric assay, based on the measurement of conversion of the yellow thiazolyl blue tetrazolium bromide (MTT) to a purple formazan derivative by mitochondrial dehydrogenase in viable cells. The HepG2 cells were cultured in *Minimum Essential Medium Eagle (MEM; Sigma)* supplemented with 10% fetal bovine serum (FBS; *Gibco*), sodium bicarbonate (1.5 g/L), sodium pyruvate (0.11 g/L), HEPES buffer (20 mM), streptomycin (0.1 g/L), and penicillin (100 000 IU/L), at 37°C in a humidified atmosphere containing 5% CO_2. For the experiments, the cells were seeded in 96-well plates at the density 25 000 cells/well in 0.2 mL of MEM 10% FBS and incubated for 24 h to attach. Then, the medium was removed and the cells were treated by samples' dilutions at the concentrations 0,000001, 0,00001, 0,0001, 0,001, and 0,01% w/v, for 24 h. Two independent experiments were conducted, and in each experiment cells were treated in triplicates, with control (nontreated) wells included in each plate. In each experiment, solvent controls were also tested, in solvent concentrations corresponding to the ones in the samples treatments. Following incubation, medium was removed and cells were incubated for 3 h with 0.05 mg/0.1 mL/well MTT dissolved in serum-free MEM. Formazan salts were dissolved in 0.1 mL/well of 0.04 M HCl in isopropanol, and light absorption was measured using a plate reader *(Thermo Labsystems)* on 540 nm, with reference wavelength 690 nm. Cell viability was expressed as a percentage of the corresponding control value (100%). The data were analyzed by one-way ANOVA, followed by *Dunnett's Multiple Comparison Test* ($P \leq 0.05$) using the *GraphPad Prism 5* software.

2.2.9. Antimicrobial Activity. The antimicrobial activity of the ZnO and PLGA/nano-ZnO particles was investigated against Gram-positive bacteria *Staphylococcus aureus* (ATCC 25923), *Staphylococcus epidermidis* (ATCC 12228), and *Bacillus subtilis* (ATCC 6633) and the Gram-negative bacteria *Escherichia coli* (ATCC 25922), *Klebsiella pneumoniae* (ATCC 13883), *Salmonella abony* (NTCT – 6017) and *Pseudomonas aeruginosa* (ATCC 27853), and the yeast *Candida albicans* (ATCC

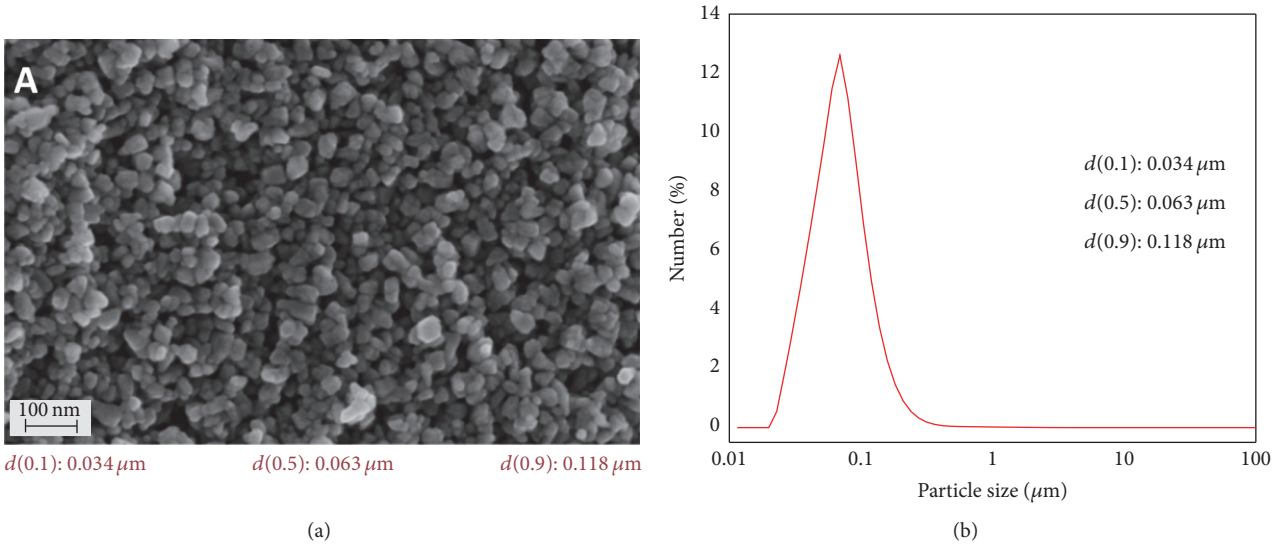

Figure 2: (a) Representative FE-SEM image of ZnO particles (bar 100 nm). (b) Particle size distribution profile for ZnO particles.

24433). In order to determine minimum inhibitory concentrations (MICs) of the prepared samples, a broth microdilution method was used. MIC represents the lowest concentration of a compound at which the microorganism does not demonstrate visible growth. MICs were determined according to Clinical and Laboratory Standards Institute (CLSI 2007) [35]. Tests were performed in Müller Hinton broth for the bacterial strains and in Sabouraud dextrose broth for *C. albicans*. Overnight broth cultures were prepared for each strain, and the final concentration in each well was adjusted to 2×106 CFU/mL. The tested samples were dissolved in 1% dimethylsulfoxide and diluted to the desired concentrations (ranging from 62,5 to 1000 μg/mL) in fresh Müller-Hinton broth for bacteria and Sabouraud broth for *C. albicans*. In the tests, 0.05% triphenyl tetrazolium chloride (TTC, Aldrich Chemical Company Inc., USA) was also added to the culture medium as a growth indicator. TTC is a redox indicator used for differentiation between metabolically active and nonactive cells. The colorless compound is enzymatically reduced to red 1,3,5-triphenylformazan by cell dehydrogenases, indicating metabolic activity (red color of the medium in microtiter plate well). As a positive control of growth, wells containing only the microorganisms in the broth were used. Bacteria growth was determined after 24 h, while growth of *Candida albicans* was determined after 48 h of incubation at 37°C. All of the MIC determinations were performed in duplicate, and two positive growth controls were included.

3. Results and Discussion

Even though the morphology of micro- and nanoparticles is of great importance, it is generally not well characterized and practically very hard to control. Nevertheless, this is of prime importance. Morphological characteristics of the obtained ZnO particles are revealed by FE-SEM and PSA. Figure 2(a) shows nanostructured ZnO powder composed of uniform, spherical particles with a narrow particle size distribution and average diameter of approximately 63 nm (Figure 2(b)). From the presented FE-SEM image (Figure 2(a)), it can be seen that obtained ZnO powder is composed of well dispersed nanoparticles. Particles size distribution of the ZnO nanopowder is presented in Figure 2(b). Designations d_{10}, d_{50}, and d_{90} means that 10, 50, and 90% of total number of the measured particles have diameter less than 34 nm, 63 nm, and 118 nm, respectively.

SEM images of PLGA/nano-ZnO particles prepared by physicochemical solvent/nonsolvent method with acetone as solvent and dried at room temperature are presented in Figure 3(A). SEM analysis showed that PLGA/nano-ZnO particles have uniform, spherical morphology, with a narrow particle size distribution and smooth surfaces. Diameters of the particles are of about 200 nm. In contrast to well defined morphology of PLGA/nano-ZnO particles prepared with acetone, PLGA/nano-ZnO particles, prepared with ethyl acetate as solvent and dried at room temperature, are very agglomerated, with no clearly defined forms and dimensions (Figure 3(B)). Only small number of spherical, micron size particles, with a broad particle size distribution and a smooth surface can be seen in the sample presented in Figure 3(B). PLGA/nano-ZnO particles prepared by physicochemical solvent/nonsolvent method with acetone as solvent and freeze-dried are presented in Figure 3(C). From these images it can be seen that sample consisted of particles which are with small sizes comparable with particle's sizes of the sample also obtained with acetone but dried at room temperature. However particles are agglomerated. Obviously, this process generates various stresses during freezing and desiccation steps. The most likely reason why particles are so agglomerated (Figure 3(C)) is that we did not use any cryoprotectant in the synthesis.

Further, we have characterized ZnO and PLGA/nano-ZnO particles prepared by physicochemical solvent/nonsolvent method with acetone as solvent and dried at room temperature. In order to determine crystal structure and

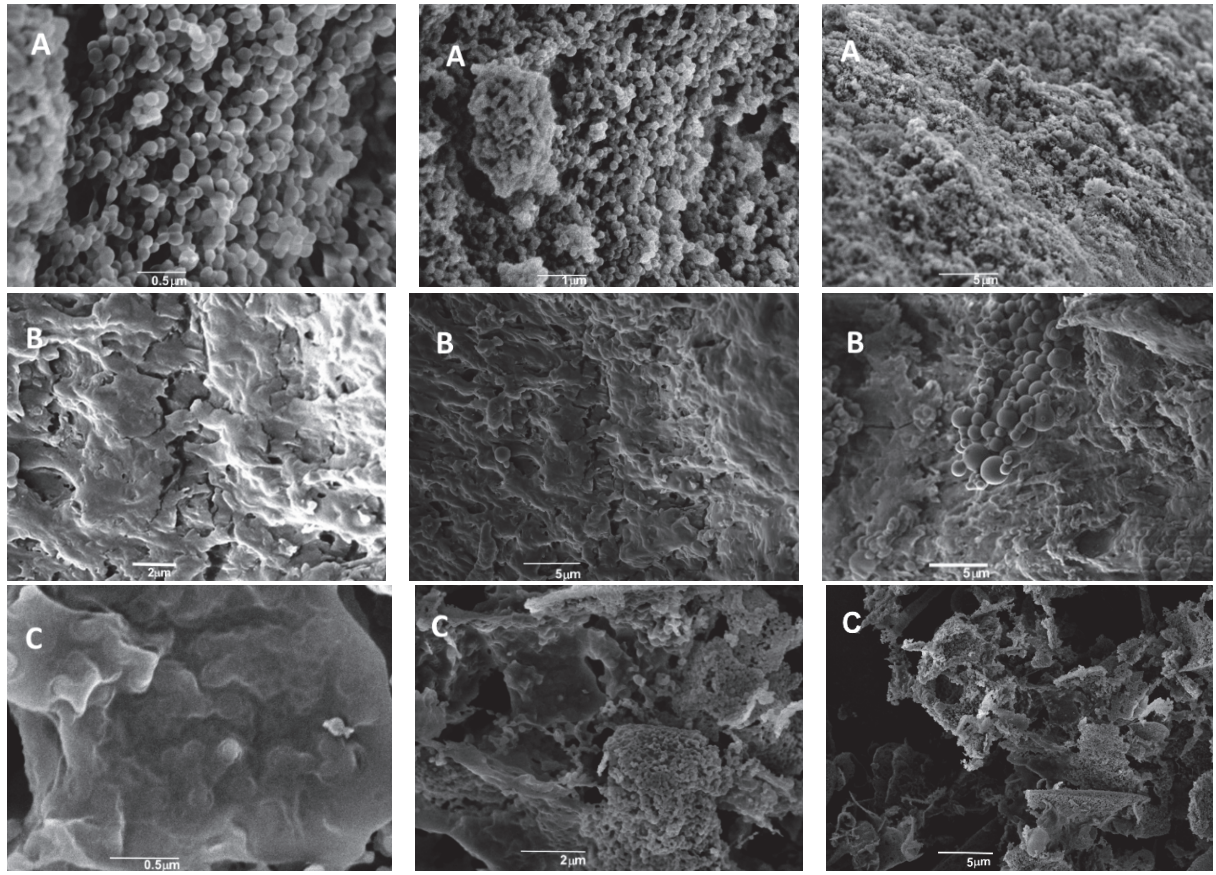

Figure 3: (A) Representative SEM images of PLGA/nano-ZnO particles prepared with acetone and dried at room temperature (bars 0,5 μm, 1 μm, and 5 μm). (B) Representative SEM images of PLGA/nano-ZnO particles prepared with ethyl acetate and dried at room temperature (bars 2 μm, 5 μm, and 5 μm). (C) Representative SEM images of PLGA/nano-ZnO particles prepared with acetone and freeze-dried (bars 0,5 μm, 2 μm, and 5 μm).

phase composition of PLGA/nano-ZnO, XRD method was applied. As it is shown in Figure 4 characteristic diffraction peaks corresponding to a pure hexagonal wurtzite phase of the crystalline ZnO nanostructured powder are obtained, according to the JCPDS card number 36-145. PLGA as an amorphous compound did not show any crystalline diffraction peaks in the presented spectra. Broad and very low intensity peak in the 2θ range of 10 to 25° was observed indicating its amorphous structure.

Figure 5(a) shows differential thermal analysis DTA (green) and relative mass loss TGA (black) curves corresponding to synthesized nanostructured ZnO powder. The TGA curve represents the total weight loss of approximately 5 wt% due to the elimination of the residual hydroxyl groups. The presence of the reaction precursor $Zn(CH_3COO)_2$ in the final product can be distinguished by the three characteristic endothermic processes that take place during heating to 350°C. The first process which corresponds to dehydration of zinc acetate dihydrate occurs at $T_1 \approx 100$°C, the second represents process of melting of anhydrous salt at $T_2 \approx 250$°C, and the third evaporation of zinc species $T_3 \approx 320$°C. The endothermic peak at $T_4 \approx 450$°C can be attributed to crystallization process of the ZnO hexagonal crystal structure [36].

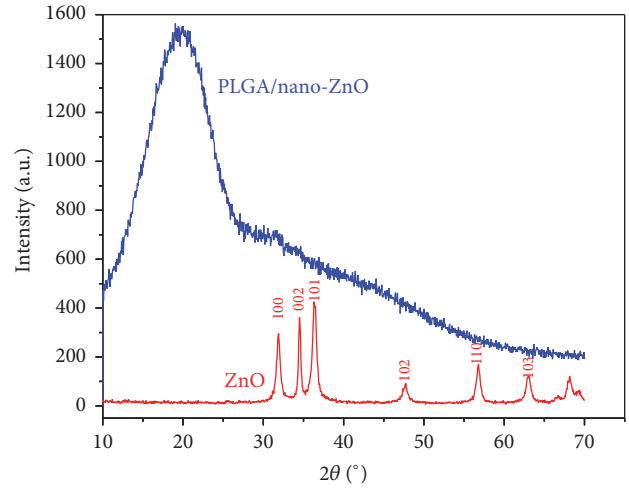

Figure 4: XRD patterns of as prepared ZnO nanoparticles and PLGA/nano-ZnO powder.

DTA-TGA curves (blue and red, resp.) of prepared PLGA/nano-ZnO powder are displayed in Figure 5(b). It can be clearly seen that the TG curve demonstrates major weight

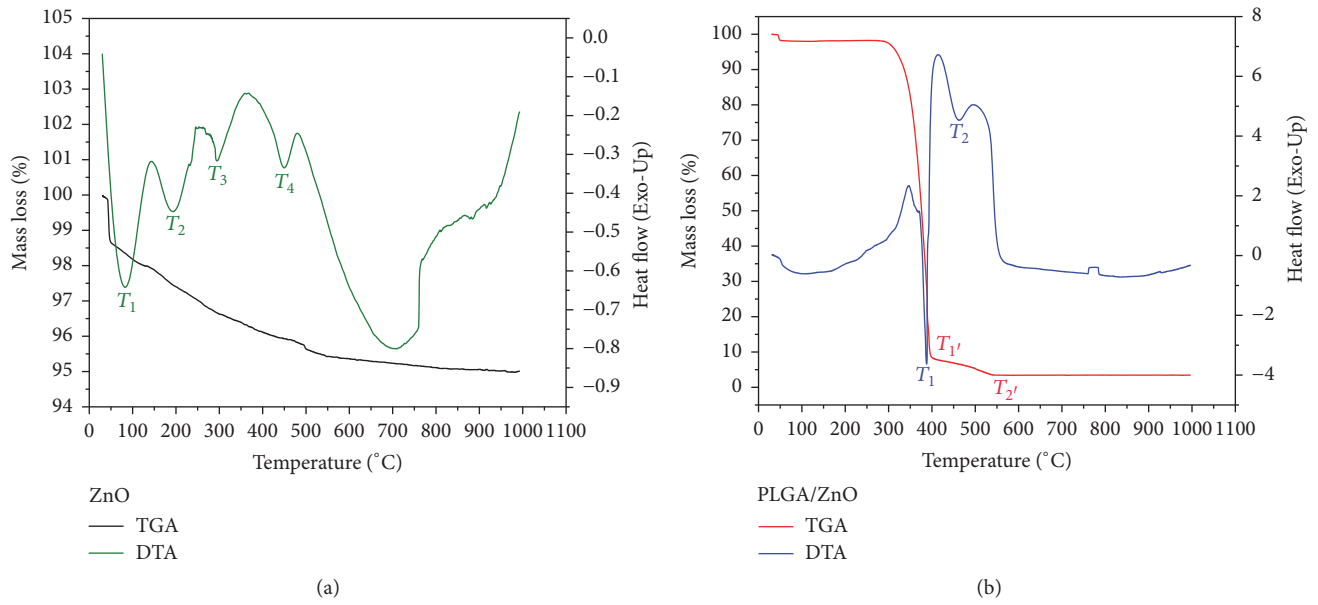

Figure 5: DTA-TGA curves of (a) ZnO nanoparticles and (b) PLGA/nano-ZnO particles prepared by physicochemical solvent/nonsolvent method with acetone as solvent and dried at room temperature.

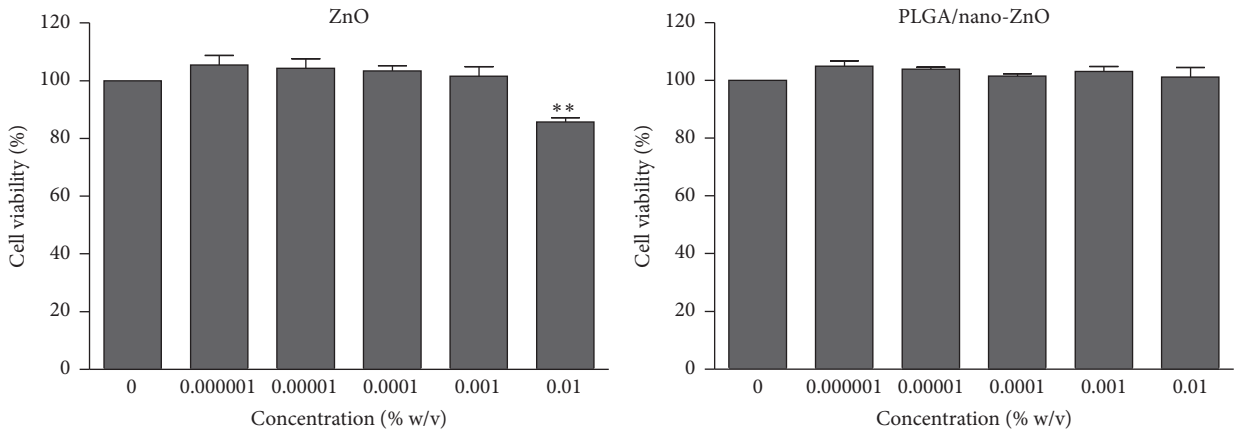

Figure 6: Viability of HepG2 cells treated with ZnO nanoparticles or PLGA/nano-ZnO for 24 h. The data are presented as mean values of six replicates from two independent experiments ±SEM. **: statistically significant difference compared to the control (0% w/v), $P \leq 0.01$.

loss of approximately 95 wt% in the considered temperature range. The weight loss of PLGA/nano-ZnO, attributed to thermal decomposition of polymer, occurs in two phases ($T_{1'} \approx 398^{\circ}$C—91. 25% and $T_{2'} \approx 545^{\circ}$C—3. 30%). DTA curve reveals an endothermic process at about 50°C which can be assigned to the relaxation peak that follows the glass transition of the polymer. The exothermic peaks around $T_1 \approx 350$, $T_2 \approx 400$, and $T_3 \approx 500^{\circ}$C are related to the thermal decomposition of the polymer. The decomposition process, characterized by an endothermic peak, has started at approximately $T \approx 320^{\circ}$C [37].

For the cytotoxicity study ZnO nanoparticles and PLGA/nano-ZnO particles prepared with acetone as solvent and ethanol as nonsolvent, were used. In vitro cytotoxicity of ZnO nanoparticles and PLGA/nano-ZnO was determined with MTT assay after exposure of HepG2 cells to 0,000001, 0,00001, 0,0001, 0,001, and 0,01% v/v of ZnO nanoparticles or of PLGA/nano-ZnO prepared with acetone for 24 h. At the applied exposure conditions ZnO nanoparticles as well as PLGA/nano-ZnO did not affect the viability of HepG2 cells (Figure 6). The cell viability data for the vehicle control are not shown in Figure 6 as they were almost identical as negative control.

One of the aims of our study was to examine antimicrobial activity of ZnO and PLGA/nano-ZnO against different groups of microorganisms (Gram-positive bacteria, Gram-negative bacteria, and yeast *Candida albicans*). In order to determine minimum inhibitory concentrations (MICs) of the tested samples we performed broth microdilution test, according to CLSI (2007) which is standard method [38]. Minimal inhibitory concentrations of the samples were determined against Gram-positive bacteria *Staphylococcus aureus*

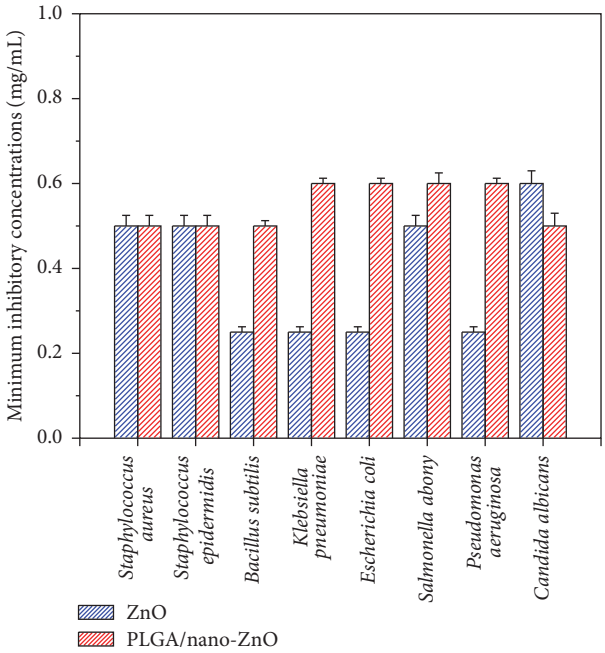

Figure 7: Minimal inhibitory concentrations of ZnO and PLGA/nano-ZnO nanoparticles determined using a broth microdilution assay against Gram-positive bacteria *Staphylococcus aureus* (ATCC 25923), *Staphylococcus epidermidis* (ATCC 12228), and *Bacillus subtilis* (ATCC 6633) and the Gram-negative bacteria *Klebsiella pneumoniae* (ATCC 13883), *Escherichia coli* (ATCC 25922), *Salmonella abony* (NTCT – 6017) and *Pseudomonas aeruginosa* (ATCC 27853), and the yeast *Candida albicans* (ATCC 24433).

(ATCC 25923), *Staphylococcus epidermidis* (ATCC 12228), and *Bacillus subtilis* (ATCC 6633) and the Gram-negative bacteria *Klebsiella pneumoniae* (ATCC 13883), *Escherichia coli* (ATCC 25922), *Salmonella abony* (NTCT – 6017) and *Pseudomonas aeruginosa* (ATCC 27853), and the yeast *Candida albicans* (ATCC 24433) (Figure 7). Generally, antimicrobial activity of nanoparticles has received significant interest worldwide since many microorganisms exist in the range from few of nanometers to tens of micrometers. One of the explanation why particles such as ZnO display antimicrobial activities is due to increased specific surface area as a result of the reduction of the particle size which leads to enhanced particle surface reactivity. Also, reactive oxygen species such as hydrogen peroxide, hydroxyl radicals, and peroxide have been important bactericidal and bacteriostatic factor for several mechanisms involving cell wall damage because of zinc oxide localized interaction, enhanced membrane permeability, internalization of nanoparticles due to loss of proton motive force, and so forth [39]. Results of this study (Figure 7) provided the evidence of a considerable antibacterial activity of ZnO as well as PLGA/nano-ZnO against all of the tested strains. The samples exhibited bacteriostatic effect. Some standard antimicrobial drugs (tetracyclines and chloramphenicol) are also, mainly, bacteriostatic, but regardless of this fact they are used in clinical practice. In this case, ZnO exhibited stronger activity against Gram-positive bacteria *Bacillus subtilis* (ATCC 6633) and the Gram-negative bacteria *Klebsiella pneumoniae* (ATCC 13883), *Escherichia coli* (ATCC 25922), and *Pseudomonas aeruginosa* (ATCC 27853) compared to the PLGA/nano-ZnO. As it is already mentioned above, the inorganic core-polymer shell hybrid microspheres have attracted attention because the materials can reveal special characteristics, such as improved strength, shape, and chemical resistance. So far, very few studies report success to preserve antibacterial activity when blended with polymer [25, 40]. Here, even if there is obviously the difference between MICs of ZnO and PLGA/nano-ZnO, particles of PLGA/nano-ZnO also showed antimicrobial properties against eight different microbial strains. From the literature it is known, in some cases, that improved antimicrobial activity of ZnO can be attributed to surface defects on its abrasive surface texture [39]. On the other hand, PLGA/nano-ZnO particles exhibited more pronounced antimicrobial activity against yeast *Candida albicans*. In the literature, different mechanisms for the microorganism and material surface interactions have been reported such as electrostatic and hydrophobic forces, van der Waals forces, and adhesins such as lectins [41]. Adhesion is an essential step for microorganism to colonize material surfaces. Previous studies described that the adhesion should be higher on hydrophobic than on hydrophilic material [41]. However, the strength of the interaction between microorganism and material depends not only on the material properties but also on the microorganism surface structure itself [42]. The differences observed for the minimum inhibitory concentrations of ZnO and PLGA/nano-ZnO when they were evaluated versus *Bacillus subtilis*, *Klebsiella pneumoniae*, *Escherichia coli*, *Salmonella abony,* and *Pseudomonas aeruginosa* can be also explained by differences in their cell envelopes. Most Gram-positive cell walls contain considerable amounts of teichoic and teichuronic acids which may account for up to 50% of the dry weight of the wall. In addition, some Gram-positive walls may contain polysaccharide molecules. Gram-negative cell walls contain three components that lie outside of the peptidoglycan layer (lipoprotein, outer membrane, and lipopolysaccharide). The permeability of the outer membrane varies widely from one Gram-negative species to another [43, 44]. In accordance with this, we observed stronger bacteriostatic activity, of tested samples, against *Klebsiella pneumoniae*, *Escherichia coli*, and *Pseudomonas aeruginosa* than against *Salmonella abony*. Although it would be good that the MIC concentrations are tested also in cytotoxicity assay, to make sure that these compounds could be used as antimicrobial without any risk, unfortunately it was not possible due to the limits of the experimental setup and great solvent concentrations that could mask the compound's effect. However, since not a single indication of cytotoxicity was observed for PLGA/nano-ZnO in 0.01% w/v concentration, we believe it is unlikely that 0.05–0.06% w/v would induce significant cytotoxic response. Our assumption can also be supported by literature data, where, for example, no cytotoxic effects of zinc containing glasses were observed at concentration of 0.5% w/v while MIC concentrations were 3-4 times lower [45]. All of the tested bacterial strains may be highly resistant to traditional antibiotic therapies [46, 47]. However, the antimicrobial mechanism is very

complex and it is not easy to fully understand the exact mechanism of cell membrane damage involved with particles. When immobilized in a polymer matrix, amount of filler, interactions between filler and polymer matrix, and particle dispersion within polymeric particles may all influence the antimicrobial activity of the material. All of this as well as kinetic release of ZnO from the PLGA polymer matrix will be the subject of our next study. Also, the subject of our future research will be to determine minimum bactericidal concentration (MBC) and influence of different external factors of antibacterial activity of ZnO and PLGA/nano-ZnO against selected bacterial strains (laboratory and clinical isolates).

4. Conclusion

Uniform, spherical ZnO particles with average diameter of 63 nm were synthesized and then successfully immobilized within a PLGA polymer matrix (PLGA/nano-ZnO). This was confirmed by X-ray diffraction, scanning electron microscopy, laser diffraction, differential thermal analysis, and thermal gravimetric analysis. Influence of different solvents as well as different drying methods on morphology of PLGA/nano-ZnO particles was evaluated. The best morphology was obtained in the case of PLGA/nano-ZnO particles prepared by physicochemical solvent/nonsolvent method with acetone as solvent and dried at room temperature. These PLGA/nano-ZnO particles are spherical in shape, uniform, and with diameters below 1 μm. The MTT assay data indicate good biocompatibility of these ZnO and PLGA/nano-ZnO. Both types of particles, ZnO and PLGA/nano-ZnO, exhibited antimicrobial inhibition activity against Gram-positive bacteria *Staphylococcus aureus*, *Staphylococcus epidermidis*, and *Bacillus subtilis* and the Gram-negative bacteria *Escherichia coli*, *Klebsiella pneumoniae*, *Salmonella abony* and *Pseudomonas aeruginosa*, and the yeast *Candida albicans*. Our data suggest that PLGA/nano-ZnO nanoparticles are promising candidates for applications in biomedical field since it is expected that such particles will demonstrate a combination of desirable properties in one device, that is, controlled drug-delivery function and prevention or elimination of possible infections.

Competing Interests

The authors declare that there is no conflict of interests regarding the publication of this paper.

Acknowledgments

The Ministry of Education, Science and Technological Development of the Republic of Serbia supported this work financially through the project Grant no. III45004. The authors would like to express gratitude to Dr. Miodrag J. Lukic for particle size distribution measurements, to MSc Nenad Filipović for the technical assistance during the experiments, and to MSc Ljljana Veselinović for performing the XRD measurements. This work is also supported by the COST Action CA15114: Anti-MIcrobial Coating Innovations to prevent infectious diseases (AMICI).

References

[1] L. S. Nair and C. T. Laurencin, "Biodegradable polymers as biomaterials," *Progress in Polymer Science*, vol. 32, no. 8-9, pp. 762–798, 2007.

[2] A. Kumari, S. K. Yadav, and S. C. Yadav, "Biodegradable polymeric nanoparticles based drug delivery systems," *Colloids and Surfaces B: Biointerfaces*, vol. 75, no. 1, pp. 1–18, 2010.

[3] P. L. Lam and R. Gambari, "Advanced progress of microencapsulation technologies: in vivo and in vitro models for studying oral and transdermal drug deliveries," *Journal of Controlled Release*, vol. 178, no. 1, pp. 25–45, 2014.

[4] H. K. Makadia and S. J. Siegel, "Poly Lactic-co-Glycolic Acid (PLGA) as biodegradable controlled drug delivery carrier," *Polymers*, vol. 3, no. 3, pp. 1377–1397, 2011.

[5] F. Danhier, E. Ansorena, J. M. Silva, R. Coco, A. Le Breton, and V. Préat, "PLGA-based nanoparticles: an overview of biomedical applications," *Journal of Controlled Release*, vol. 161, no. 2, pp. 505–522, 2012.

[6] T. K. Dash and V. B. Konkimalla, "Poly-ϵ-caprolactone based formulations for drug delivery and tissue engineering: a review," *Journal of Controlled Release*, vol. 158, pp. 15–33, 2012.

[7] M. M. Stevanović, S. D. Škapin, I. Bračko et al., "Poly(lactide-co-glycolide)/silver nanoparticles: synthesis, characterization, antimicrobial activity, cytotoxicity assessment and ROS-inducing potential," *Polymer*, vol. 53, no. 14, pp. 2818–2828, 2012.

[8] M. Stevanović, N. Filipović, J. Djurdjević, M. Lukić, M. Milenković, and A. Boccaccini, "45S5Bioglass®-based scaffolds coated with selenium nanoparticles or with poly(lactide-co-glycolide)/selenium particles: processing, evaluation and antibacterial activity," *Colloids and Surfaces B: Biointerfaces*, vol. 132, pp. 208–215, 2015.

[9] H. Hong, J. Shi, Y. Yang et al., "Cancer-targeted optical imaging with fluorescent zinc oxide nanowires," *Nano Letters*, vol. 11, no. 9, pp. 3744–3750, 2011.

[10] H.-J. Zhang, H.-M. Xiong, Q.-G. Ren, Y.-Y. Xia, and J.-L. Kong, "ZnO@silica core–shell nanoparticles with remarkable luminescence and stability in cell imaging," *Journal of Materials Chemistry*, vol. 22, no. 26, pp. 13159–13165, 2012.

[11] A. A. Ansari, A. Kaushik, P. R. Solanki, and B. D. Malhotra, "Nanostructured zinc oxide platform for mycotoxin detection," *Bioelectrochemistry*, vol. 77, no. 2, pp. 75–81, 2010.

[12] K. C. Barick, S. Nigam, and D. Bahadur, "Nanoscale assembly of mesoporous ZnO: a potential drug carrier," *Journal of Materials Chemistry*, vol. 20, no. 31, pp. 6446–6452, 2010.

[13] F. Muhammad, M. Guo, Y. Guo et al., "Acid degradable ZnO quantum dots as a platform for targeted delivery of an anticancer drug," *Journal of Materials Chemistry*, vol. 21, no. 35, pp. 13406–13412, 2011.

[14] H. Zhang, B. Chen, H. Jiang, C. Wang, H. Wang, and X. Wang, "A strategy for ZnO nanorod mediated multi-mode cancer treatment," *Biomaterials*, vol. 32, no. 7, pp. 1906–1914, 2011.

[15] D. Guo, C. Wu, H. Jiang, Q. Li, X. Wang, and B. Chen, "Synergistic cytotoxic effect of different sized ZnO nanoparticles and daunorubicin against leukemia cancer cells under UV irradiation," *Journal of Photochemistry and Photobiology B: Biology*, vol. 93, no. 3, pp. 119–126, 2008.

[16] A. Stanković, S. Dimitrijević, and D. Uskoković, "Influence of size scale and morphology on antibacterial properties of ZnO powders hydrothemally synthesized using different surface stabilizing agents," *Colloids and Surfaces B: Biointerfaces*, vol. 102, pp. 21–28, 2013.

[17] M. Stevanović, I. Bračko, M. Milenković et al., "Multifunctional PLGA particles containing poly(l-glutamic acid)-capped silver nanoparticles and ascorbic acid with simultaneous antioxidative and prolonged antimicrobial activity," *Acta Biomaterialia*, vol. 10, no. 1, pp. 151–162, 2014.

[18] E. Tang and S. Dong, "Preparation of styrene polymer/ZnO nanocomposite latex via miniemulsion polymerization and its antibacterial property," *Colloid and Polymer Science*, vol. 287, no. 9, pp. 1025–1032, 2009.

[19] D.-G. Yu and J. H. An, "Preparation and characterization of titanium dioxide core and polymer shell hybrid composite particles prepared by two-step dispersion polymerization," *Polymer*, vol. 45, no. 14, pp. 4761–4768, 2004.

[20] M. Xiong, L. Wu, S. Zhou, and B. You, "Preparation and characterization of acrylic latex/nano-SiO_2 composites," *Polymer International*, vol. 51, no. 8, pp. 693–698, 2002.

[21] Y. Zhang, X. Wang, Y. Liu, S. Song, and D. Liu, "Highly transparent bulk PMMA/ZnO nanocomposites with bright visible luminescence and efficient UV-shielding capability," *Journal of Materials Chemistry*, vol. 22, no. 24, pp. 11971–11977, 2012.

[22] G. Gedda, H. N. Abdelhamid, M. S. Khan, and H.-F. Wu, "ZnO nanoparticle-modified polymethyl methacrylate-assisted dispersive liquid-liquid microextraction coupled with MALDI-MS for rapid pathogenic bacteria analysis," *RSC Advances*, vol. 4, no. 86, pp. 45973–45983, 2014.

[23] J. Zhou, Y. Gu, P. Fei et al., "Flexible piezotronic strain sensor," *Nano Letters*, vol. 8, no. 9, pp. 3035–3040, 2008.

[24] P. Liu, "Facile preparation of monodispersed core/shell zinc oxide@polystyrene (ZnO@PS) nanoparticles via soapless seeded microemulsion polymerization," *Colloids and Surfaces A: Physicochemical and Engineering Aspects*, vol. 291, no. 1–3, pp. 155–161, 2006.

[25] G. Droval, I. Aranberri, L. Germán et al., "Thermal and rheological characterization of antibacterial nanocomposites: poly(amide) 6 and low-density poly(ethylene) filled with zinc oxide," *Journal of Thermoplastic Composite Materials*, vol. 27, no. 2, pp. 268–284, 2014.

[26] Y.-Y. Chen, C.-C. Kuo, B.-Y. Chen, P.-C. Chiu, and P.-C. Tsai, "Multifunctional polyacrylonitrile-ZnO/Ag electrospun nanofiber membranes with various ZnO morphologies for photocatalytic, UV-shielding, and antibacterial applications," *Journal of Polymer Science Part B: Polymer Physics*, vol. 53, no. 4, pp. 262–269, 2015.

[27] T. Amna, M. S. Hassan, F. A. Sheikh et al., "Zinc oxide-doped poly(urethane) spider web nanofibrous scaffold via one-step electrospinning: a novel matrix for tissue engineering," *Applied Microbiology and Biotechnology*, vol. 97, no. 4, pp. 1725–1734, 2013.

[28] S. Awad, H. Chen, G. Chen et al., "Free volumes, glass transitions, and cross-links in zinc oxide/waterborne polyurethane nanocomposites," *Macromolecules*, vol. 44, no. 1, pp. 29–38, 2011.

[29] A. Kołodziejczak-Radzimska and T. Jesionowski, "Zinc oxide—from synthesis to application: a review," *Materials*, vol. 7, no. 4, pp. 2833–2881, 2014.

[30] Y.-S. Park, K.-N. Kim, K.-M. Kim et al., "Feasibility of three-dimensional macroporous scaffold using calcium phosphate glass and polyurethane sponge," *Journal of Materials Science*, vol. 41, no. 13, pp. 4357–4364, 2006.

[31] T. Kos, A. Anžlovar, D. Pahovnik, E. Žagar, Z. C. Orel, and M. Žigon, "Zinc-containing block copolymer as a precursor for the in situ formation of nano ZnO and PMMA/ZnO nanocomposites," *Macromolecules*, vol. 46, no. 17, pp. 6942–6948, 2013.

[32] J. T. Seil and T. J. Webster, "Reduced *Staphylococcus aureus* proliferation and biofilm formation on zinc oxide nanoparticle PVC composite surfaces," *Acta Biomaterialia*, vol. 7, no. 6, pp. 2579–2584, 2011.

[33] Q. Peng, Y.-C. Tseng, S. B. Darling, and J. W. Elam, "A route to nanoscopic materials via sequential infiltration synthesis on block copolymer templates," *ACS Nano*, vol. 5, no. 6, pp. 4600–4606, 2011.

[34] S. Marković, V. Rajić, A. Stanković et al., "Effect of PEO molecular weight on sunlight induced photocatalytic activity of ZnO/PEO composites," *Solar Energy*, vol. 127, pp. 124–135, 2016.

[35] Clinical and Laboratory Standards Institute (CLSI), "Performance standards for antimicrobial susceptibility testing: 17th informational supplement," CLSI Document M100-S17, CLSI, Wayne, Pa, USA, 2007.

[36] M. S. Tokumoto, S. H. Pulcinelli, C. V. Santilli, and V. Briois, "Catalysis and temperature dependence on the formation of ZnO nanoparticles and of zinc acetate derivatives prepared by the sol-gel route," *Journal of Physical Chemistry B*, vol. 107, no. 2, pp. 568–574, 2003.

[37] R. M. Mainardes, M. P. D. Gremião, and R. C. Evangelista, "Thermoanalytical study of praziquantel-loaded PLGA nanoparticles," *Revista Brasileira de Ciencias Farmaceuticas/Brazilian Journal of Pharmaceutical Sciences*, vol. 42, no. 4, pp. 523–530, 2006.

[38] G. Brađan, A. Pevec, I. Turel et al., "Synthesis, characterization, DFT calculations and antimicrobial activity of pentagonal-bipyramidal Zn(II) and Cd(II) complexes with 2,6-diacetylpyridine-bis(trimethylammoniumacetohydrazone)," *Journal of Coordination Chemistry*, vol. 69, no. 18, pp. 2754–2765, 2016.

[39] S. Amna, M. Shahrom, S. Azman et al., "Review on zinc oxide nanoparticles: antibacterial activity and toxicity mechanism," *Nano-Micro Letters*, vol. 7, no. 3, pp. 219–242, 2015.

[40] J. H. Li, R. Y. Hong, M. Y. Li, H. Z. Li, Y. Zheng, and J. Ding, "Effects of ZnO nanoparticles on the mechanical and antibacterial properties of polyurethane coatings," *Progress in Organic Coatings*, vol. 64, no. 4, pp. 504–509, 2009.

[41] A. Al-Ahmad, M. Wiedmann-Al-Ahmad, C. Carvalho et al., "Bacterial and *Candida albicans* adhesion on rapid prototyping-produced 3D-scaffolds manufactured as bone replacement materials," *Journal of Biomedical Materials Research—Part A*, vol. 87, no. 4, pp. 933–943, 2008.

[42] Y. H. An and R. J. Friedman, "Concise review of mechanisms of bacterial adhesion to biomaterial surfaces," *Journal of Biomedical Materials Research*, vol. 43, no. 3, pp. 338–348, 1998.

[43] G. F. Brooks, K. C. Carroll, J. S. Butel, S. A. Morse, and T. A. Mietzner, *Jawetz, Melnick & Adelberg's Medical Microbiology*, chapter 2, McGraw-Hill, 26th edition, 2013.

[44] P. R. Murray, K. S. Rosenthal, and M. A. Pfaller, *Bacterial Classification, Structure, and Replication, Medical Microbiology*, Elsevier, 7th edition, 2013.

[45] L. Esteban-Tejeda, C. Prado, B. Cabal, J. Sanz, R. Torrecillas, and J. S. Moya, "Antibacterial and antifungal activity of ZnO

containing glasses," *PLoS ONE*, vol. 10, no. 7, Article ID e0132709, 2015.

[46] M. Stevanović, V. Uskoković, M. Filipović, S. D. Škapin, and D. Uskoković, "Composite PLGA/AgNpPGA/AscH nanospheres with combined osteoinductive, antioxidative, and antimicrobial activities," *ACS Applied Materials and Interfaces*, vol. 5, no. 18, pp. 9034–9042, 2013.

[47] E. Oldfield and X. Feng, "Resistance-resistant antibiotics," *Trends in Pharmacological Sciences*, vol. 35, no. 12, pp. 664–674, 2014.